JVI Journals.ASM.org

Enhanced Transgene Expression from Recombinant Single-Stranded D-Sequence-Substituted Adeno-Associated Virus Vectors in Human Cell Lines *In Vitro* and in Murine Hepatocytes *In Vivo*

Chen Ling,[a,b] Yuan Wang,[a,b,c,d] Yuan Lu,[e] Lina Wang,[a,b,c] Giridhara R. Jayandharan,[f]* George V. Aslanidi,[a,b] Baozheng Li,[a,b] Binbin Cheng,[a,c] Wenqin Ma,[a,b] Thomas Lentz,[g] Changquan Ling,[c,d] Xiao Xiao,[g,h] R. Jude Samulski,[g] Nicholas Muzyczka,[b,i,j] Arun Srivastava[a,b,i,j,k]

Division of Cellular and Molecular Therapy, Department of Pediatrics,[a] Powell Gene Therapy Center,[b] Department of Orthopedics & Rehabilitative Medicine,[e] Department of Molecular Genetics & Microbiology,[i] Genetics Institute,[j] and Shands Cancer Center,[k] University of Florida College of Medicine, Gainesville, Florida, USA; Division of Molecular Pharmaceutics, University of North Carolina School of Pharmacy, Chapel Hill, North Carolina, USA[h]; Gene Therapy Center, University of North Carolina at Chapel Hill, Chapel Hill, North Carolina, USA[g]; Department of Traditional Chinese Medicine, Changhai Hospital, Second Military Medical University, Shanghai, China[c]; Shanghai University of Traditional Chinese Medicine, Shanghai, China[d]; Department of Haematology, and Centre for Stem Cell Research, Christian Medical College, Vellore, India[f]

ABSTRACT

We have previously reported that the removal of a 20-nucleotide sequence, termed the D sequence, from both ends of the inverted terminal repeats (ITRs) in the adeno-associated virus serotype 2 (AAV2) genome significantly impairs rescue, replication, and encapsidation of the viral genomes (X. S. Wang, S. Ponnazhagan, and A. Srivastava, J Mol Biol 250:573–580, 1995; X. S. Wang, S. Ponnazhagan, and A. Srivastava, J Virol 70:1668–1677, 1996). Here we describe that replacement of only one D sequence in either ITR restores each of these functions, but DNA strands of only single polarity are encapsidated in mature progeny virions. Since most commonly used recombinant AAV vectors contain a single-stranded DNA (ssDNA), which is transcriptionally inactive, efficient transgene expression from AAV vectors is dependent upon viral second-strand DNA synthesis. We have also identified a transcription suppressor sequence in one of the D sequences, which shares homology with the binding site for the cellular NF-κB-repressing factor (NRF). The removal of this D sequence from, and replacement with a sequence containing putative binding sites for transcription factors in, single-stranded AAV (ssAAV) vectors significantly augments transgene expression both in human cell lines *in vitro* and in murine hepatocytes *in vivo*. The development of these genome-modified ssAAV vectors has implications not only for the basic biology of AAV but also for the optimal use of these vectors in human gene therapy.

IMPORTANCE

The results of the studies described here not only have provided novel insights into some of the critical steps in the life cycle of a human virus, the adeno-associated virus (AAV), that causes no known disease but have also led to the development of novel recombinant AAV vectors which are more efficient in allowing increased levels of gene expression. Thus, these studies have significant implications for the potential use of these novel AAV vectors in human gene therapy.

The wild-type (WT) adeno-associated virus (AAV) is a nonpathogenic member of the *Parvoviridae* family with a 4.7-kb single-stranded DNA (ssDNA) genome (1). It has gained particular attention because recombinant AAV (rAAV) vectors represent one of the most promising viral vector systems for gene therapy (2) and are currently in use in a number of gene therapy clinical trials (3). Most rAAV vectors used in clinical trials are single-stranded vectors. We and others have demonstrated that viral second-strand DNA synthesis is one of the major rate-limiting steps in single-stranded AAV (ssAAV) vector-mediated transgene expression (4–7). Recently, the development of self-complementary AAV (scAAV) vectors, which can bypass the requirement of viral second-strand DNA synthesis (8–10), has shown remarkable efficacy in the treatment of hemophilia B patients (11). However, a major limitation of scAAV vectors is their packaging capacity, which is ~2.5 kb. Such a limited packaging capacity excludes many larger therapeutic genes. When common promoters such as the cytomegalovirus (CMV) promoter and chicken β-actin (CBA) promoter are used, a cDNA of less than 1.2 kb can be packaged into the scAAV vectors. The inclusion of many tissue-specific promoters, such as the human alpha-1 antitrypsin (hAAT) promoter, further excludes many therapeutic genes, for instance, the human factor VIII gene (12). Therefore, strategies to improve the transduction efficiency of conventional ssAAV vectors are needed.

Both WT and rAAV genomes contain inverted terminal repeats (ITRs) of 145 nucleotides (nt) at both ends. The terminal 125 nucleotides in each ITR form a palindromic double-stranded

Received 8 September 2014 **Accepted** 20 October 2014

Accepted manuscript posted online 29 October 2014

Citation Ling C, Wang Y, Lu Y, Wang L, Jayandharan GR, Aslanidi GV, Li B, Cheng B, Ma W, Lentz T, Ling C, Xiao X, Samulski RJ, Muzyczka N, Srivastava A. 2015. Enhanced transgene expression from recombinant single-stranded D-sequence-substituted adeno-associated virus vectors in human cell lines *in vitro* and in murine hepatocytes *in vivo*. J Virol 89:952–961. doi:10.1128/JVI.02581-14.

Editor: M. J. Imperiale

Address correspondence to Chen Ling, lingchen@peds.ufl.edu, or Arun Srivastava, aruns@peds.ufl.edu.

* Present address: Giridhara R. Jayandharan, Department of Biological Sciences and Bioengineering, Indian Institute of Technology, Kanpur, UP, India.

C.L. and Y.W. contributed equally to this article.

doi:10.1128/JVI.02581-14

T-shaped hairpin structure (1), in which the A-A′ palindrome forms the stem and the two smaller palindromes, B-B′ and C-C′, form the cross-arms of the T. The other 20 nucleotides (D sequence) in the ITR remain single stranded. The ssD[−] sequence is always at the 3′ end, whereas the complementary one, the ssD[+] sequence is invariably at the 5′ end. Once in the cells, the single-stranded genome undergoes second-strand DNA synthesis, which turns both the ssD[−] and ssD[+] sequences into double-stranded D[±] (dsD[±]) sequences. Our laboratory has previously documented that phosphorylated forms of a 52-kDa cellular chaperone protein, FKBP52 (FK506-binding protein), specifically interact with the ssD[−] sequence and hence inhibit viral second-strand DNA synthesis and subsequent transgene expression (7, 13–15). On the other hand, dephosphorylation of FKBP52 at tyrosine residues by the cellular T-cell protein tyrosine phosphatase (TC-PTP) and at serine/threonine residues by protein phosphatase 5 (PP5) prevents FKBP52 from binding to the ssD[−] sequence, leading to efficient viral second-strand DNA synthesis (14, 16).

What role the ssD[+] sequence plays during the life cycle of AAV still remains unclear, although we have previously demonstrated the existence of a cellular protein which specifically interacts with the ssD[+]-sequence probe (6). Following purification and mass spectrometry, the cellular protein binding with the ssD[+] sequence was found to have partial amino acid homology to NF-κB-repressing factor (NRF), a negative regulator of transcription (NRF) (17). Since both the cellular proteins binding with either the ssD[−] or ssD[+] sequence have the potential to inhibit transgene expression mediated by ssAAV vectors and since we have previously reported that the removal of the D sequences from the viral genome impairs rescue, replication, and encapsidation of AAV DNA (18–20), we wished to examine whether restoration of one D sequence in the ssAAV genome might not only restore rescue, replication, and encapsidation but also enhance transgene expression from ssAAV vectors. We report here that the ssD[+]-sequence-substituted ssAAV genomes could be successfully packaged into rAAV vectors and that the transduction efficiency of these vectors was significantly higher than that of conventional ssAAV vectors.

MATERIALS AND METHODS

Cell lines, DNA primers, and ^{32}P-labeled probes. Human cervical cancer (HeLa), embryonic kidney (HEK293), and osteosarcoma (U2OS) cells were purchased from American Type Culture Collection (Manassas, VA, USA). Human hepatocellular carcinoma (Huh7) cells were described previously (21). All cells were maintained in complete Dulbecco modified Eagle medium (C-DMEM) (Mediatech Inc., Manassas, VA, USA) supplemented with 10% heat-inactivated fetal bovine serum (FBS) (Sigma-Aldrich, St. Louis, MO, USA) and 1% penicillin and streptomycin (P/S) (Lonza, Walkersville, MD). Cells were grown as adherent cultures in a humidified atmosphere at 37°C in 5% CO_2, subcultured after treatment with trypsin-Versene mixture (Lonza, Walkersville, MD) for 2 to 5 min at room temperature (RT), washed, and resuspended in complete medium.

Primer pairs specific for CMVenhancer-F (5′-TCCCATAGTAACGC CAATAGG-3′) and CMVenhancer-R (5′-CTTGGCATATGATACACTT GATG-3′) were used in encapsidation assays. EcoRI- and XhoI-doubly digested or XhoI- and RsrII-doubly digested plasmids pAAV-hrGFP, followed by gel recovery, were used as DNA templates to generate ^{32}P-labled humanized recombinant green fluorescent protein (hrGFP) and hGH(A)n probes, respectively. Briefly, DNA templates were denatured by heating for 10 min at 100°C, followed by rapid chilling in an ice bath. Random-primed labeling was performed using Klenow enzyme (Roche, Indianapolis, IN, USA) following the manufacturer's instructions. ^{32}P-labeled probes were then purified with a MicrospinTM G-50 column (GE Healthcare, Piscataway, NJ, USA). To determine the polarity of the AAV vector genomes, two sets of identical slot blot membranes were hybridized separately with each one of the following two complementary oligonucleotides derived from hrGFP: probe hrGFP(+), 5′-GGGGAAGCTCTGGA TGAAGAAGTCGCT-3′, and probe hrGFP(−), 5′-AGCGACTTCTTCA TCCAGAGCTTCCCC-3′. The oligonucleotides were labeled prior to the hybridization using the digoxigenin (DIG) oligonucleotide 3′-end-labeling kit (Roche, Indianapolis, IN, USA) as per the manufacturer's instructions.

AAV DNA rescue and replication assays. Equivalent amounts of each of the recombinant AAV plasmids were transfected in HEK293 cells together with pACG2 and pHelper by the triple-plasmid transfection protocol. At 72 h posttransfection, low-M_r DNA samples were isolated by the procedure described by Hirt (22) and digested extensively with DpnI at 100 U/ml for 2 h in a buffer containing 50 mM potassium acetate, 20 mM Tris-acetate, 10 mM magnesium acetate, and 1 mM dithiothreitol (DTT). DpnI-treated samples were analyzed on Southern blots using ^{32}P-labeled DNA probes specific for the hrGFP.

AAV DNA encapsidation assays. Equivalent amounts of each of the recombinant AAV plasmids were transfected together with pACG2 and pHelper by the triple-plasmid transfection protocol in HEK293 cells in 6-well plates. Cells were harvested at 72 h posttransfection, subjected to 3 rounds of freeze-thawing, and then digested with 50 U/ml Benzonase (EMD Millipore, Darmstadt, Germany) at 37°C for 1 h. Cell lysates were then centrifuged at 4,000 rpm for 30 min. Equivalent amounts of supernatants were deproteinized to release the rAAV genomes by incubation at 65°C for 30 min in NaOH at a final concentration of 100 mM. The viral DNA was purified with the DNA Clean & Concentrator-5 kit (Zymo Research, Irvine, CA, USA) and subjected to quantitative PCR (qPCR) assays.

Recombinant AAV vectors. Highly purified stocks of AAV2 vectors, containing a CMV promoter driving the hrGFP expression gene or containing a CBA promoter driving the firefly luciferase expression gene, were packaged by the triple-plasmid transfection protocol (23, 24). Briefly, HEK293 cells were cotransfected with three plasmids using polyethylenimine (PEI) (linear; molecular weight [MW], 25,000) (Polysciences, Inc., Warrington, PA), and medium was replaced at 6 h posttransfection. Cells were harvested at 72 h posttransfection, subjected to 3 rounds of freeze-thawing, and then digested with 100 U/ml Benzonase (EMD Millipore, Darmstadt, Germany) at 37°C for 1 h. Viral vectors were purified by iodixanol (Sigma, St. Louis, MO) gradient ultracentrifugation followed by ion-exchange chromatography using HiTrap Q HP (GE Healthcare, Piscataway, NJ), washed with phosphate-buffered saline (PBS), and concentrated by centrifugation using centrifugal spin concentrators with a 150,000-molecular-weight cutoff (MWCO). Viral vectors were resuspended in 500 μl PBS.

Quantitative DNA slot blot analyses. The physical genomic titers of recombinant vector stocks were determined by quantitative DNA slot blot analysis as previously described (25). Briefly, 10 μl vector stocks was digested with 100 U/ml Benzonase (EMD Millipore, Darmstadt, Germany) at 37°C for 1 h. An equal volume of 200 mM NaOH was added, followed by incubation at 65°C for 30 min. A known quantity of plasmid DNA was also treated in the same manner for use as a standard reference during quantitation. DNA samples were loaded in 2-fold serial dilutions onto Immobilon-NY+ membranes (Millipore, Bedford, MA). After cross-linking, the membranes were then prehybridized for 6 h at 68°C in 25 ml hybridization solution containing 6× SSC (1× SSC is 0.15 M NaCl plus 0.015 M sodium citrate), 100 μg/ml freshly boiled herring sperm DNA, 0.5% sodium dodecyl sulfate (SDS), and 5× Denhardt's reagent. Subsequently, the membranes were hybridized with freshly boiled ^{32}P-labeled DNA probe in a total volume of 25 ml of hybridization solution at 68°C for 18 to 20 h. Membranes were then washed once in 50 ml wash solution 1 (2× SSC, 0.1% SDS) at RT for 15 min and twice in 50 ml wash solution 2

(0.1× SSC, 0.1% SDS) at 68°C for 30 min and then exposed to Biomax MRTM X-ray films (Kodak, Rochester, NY) at −70°C.

Southern blot analyses. The viral DNA samples isolated from AAV DNA rescue and replication assays were purified with the DNA Clean & Concentrator-5 kit (Zymo Research, Irvine, CA, USA), dissolved in 20 μl double-distilled water (ddH_2O), and electrophoresed on 1.2% neutral agarose gels. DNA was transferred to nylon membranes. Briefly, the gel was equilibrated at RT with solution I (0.25 M HCl) for 20 min, solution II (1 M NaCl, 0.5 M NaOH) for 40 min, and solution III (1 M NaCl, 0.5 M Tris-HCl) for 40 min. The DNA was transferred to Immobilon-NY+ membranes (Millipore, Bedford, MA) in 20× SSC. After UV cross-linking, the membranes were treated as described above.

Western blot assays. Western blot assays were performed as previously described (26). Briefly, viral stocks were boiled for 10 min with loading buffer, electrophoresed using 12% SDS-PAGE, electrotransferred to nitrocellulose membranes (Bio-Rad), and probed with antibody B1 (ARP, Waltham, MA, USA) at 4°C overnight. The membranes were then incubated with horseradish peroxidase-conjugated secondary antibodies (1:5,000 dilution; GE Healthcare, Piscataway, NJ, USA) and detected with an enhanced chemiluminescence substrate (MEMD Millipore, Billerica, MA, USA).

Recombinant AAV vector transduction *in vitro*. Cells were seeded in 96-well plates at 10,000 cells per well in C-DMEM. AAV infections were performed in serum- and antibiotic-free DMEM for 2 h, followed by extensive washes with PBS to remove the vector inoculum. Transgene expression was analyzed by fluorescence microscopy at 72 h posttransduction. Alternatively, transgene expression was also analyzed by flow cytometry at 72 h posttransduction.

Animal handling. All animal experiments were performed according to the guidelines for animal care specified by the Animal Care Services at the University of Florida (Gainesville, FL). Six- to 10-week-old C57BL/6J male mice were purchased from Jackson Laboratory (Bar Harbor, ME) and maintained at the University of Florida College of Medicine (Gainesville, FL). The Institutional Animal Care and Use Committee approved all protocols for the care and use of these mice.

Recombinant AAV vector transduction *in vivo*. Recombinant ssAAV2 vectors were injected intravenously via the tail vein into C57BL/6J mice at 1×10^{10} vector genomes (vgs) per animal. Phosphate-buffered saline (PBS)-injected mice were used as an appropriate control. For the fluorescence reporter gene, mice livers were harvested at 2, 4, and 6 weeks after vector administration, and thin sections from each hepatic lobe were mounted on slides and visualized under a fluorescence microscope. For the luciferase reporter gene, *in vivo* Fluc imaging was done as described previously (27). Briefly, mice were weighed to calculate the volume of substrate according to the dose of 4 mg/kg of body weight and anesthetized. The calculated volume of the 5-mg/ml stock substrate solution was mixed with 100 μl of PBS and injected via the intraperitoneal route. *In vivo* bioluminescence imaging was acquired immediately over a period of 5 min using a Xenogen machine equipped with a cooled charge-coupled device camera (Xenogen, Alameda CA). Signal intensity was quantified using the camera control program, Living Image software, and shown as photons/second/cm^2/steridian (p/s/cm^2/sr).

Statistical analysis. Results are presented as mean ± standard deviation (SD). Differences between groups were identified using a grouped unpaired two-tailed distribution of Student's *t* test. *P* values of <0.05 were considered statistically significant.

RESULTS

One D sequence restores rescue, replication, and encapsidation of recombinant AAV genomes. To examine the consequences of replacement of the D sequence in either ITR, the following two plasmids containing the identical expression cassette of a CMV promoter-driven humanized recombinant green fluorescent protein (hrGFP), flanked by two wild-type (WT) AAV2 ITRs of 145 nucleotides (Fig. 1A, top), were constructed: (i) pLC1-hrGFP, in which the D sequence in the left ITR was replaced with a non-AAV substitute (S) sequence (Fig. 1A, middle), and (ii) pLC2-hrGFP, in which the D sequence in the right ITR was replaced with the S sequence (Fig. 1A, bottom). The S sequence was chosen due to the fact that this specific oligonucleotide does not interact with the cellular proteins that bind with the D sequences (6), and that the S sequence does not compete with the D sequence (20). In addition, in each of the rAAV genomes, the terminal resolution sites (*trs*) in both ITRs remain functional (18–20), and the entire vector genome size is larger than 2.8 kb, which exceeds the packaging capacity of self-complementary AAV (scAAV) vectors (9, 10), to ensure that only virions containing ssAAV genomes were packaged (28–30).

Recombinant AAV genome rescue and replication assays were performed following cotransfection of these plasmids separately into HEK293 cells with AAV (pACG2) and adenovirus helper (pHelper) plasmids. Low-M_r DNA samples were isolated at various time points posttransfection, extensively digested with DpnI, and analyzed on Southern blots using a ^{32}P-labeled hrGFP-specific DNA probe. These results are shown in Fig. 1B. The kinetics of rAAV genome rescue and replication from both mutant plasmids pLC1-hrGFP and pLC2-hrGFP were nearly the same as that from pAAV-hrGFP, as determined by time-dependent accumulation of monomeric (m) and dimeric (d) forms of rAAV DNA replicative intermediates, albeit less efficiently. These results nonetheless suggest that the presence of one D sequence in either of the two ITRs is necessary and sufficient for the rescue and replication of the rAAV genomes. These results further corroborate that the *trs* in each of the D-sequence-substituted genomes was functional, since both m and d forms of rAAV DNA replicative intermediates were detected, in contrast to the accumulation of only duplex DNA that occurs when scAAV vectors are used, which have a mutation in one *trs* (10).

The S sequence is retained during AAV DNA rescue and replication. Since previous studies have shown that one ITR can serve as a template to repair the other ITR during AAV DNA rescue and replication (31), it was important to determine whether the D sequence in one ITR displaced the S sequence in the other ITR. To this end, low-M_r DNA samples isolated at 72 h posttransfection were digested with DpnI, followed by digestion with or without BglII restriction endonuclease. The schematic structures of various DNA replicative intermediates are depicted in Fig. 1D. The S sequence contains an additional BglII site, and following digestion with BglII, the WT and the D-sequence-substituted AAV genomes would be expected to produce unique sets of restriction fragments that are consistent with the presence of both tail-to-tail (T-T) and head-to-head (H-H) configurations, provided that the S sequence is not repaired. Southern blot analysis of BglII-digested DNA fragments using a ^{32}P-labeled probe specific for hrGFP produced the expected bands of 2.11 kb and 4.22 kb for pAAV-hrGFP (Fig. 1C, lane 6). Similarly, a band of 1.968 kb for pLC1 (Fig. 1C, lane 4) and two bands of 2.155 kb and 4.31 kb for pLC2 (Fig. 1C, lane 5) were also detected. In addition, the presence of the expected DNA bands (Fig. 1D) in each corresponding group demonstrated that the S sequence was retained during viral DNA replication. These results demonstrate that the S sequence in viral replicative DNA intermediates derived from pLC1 and pLC2 is not repaired during rescue and replication.

One D sequence restores encapsidation of the mutant AAV genomes. To examine whether the viral genomes rescued and

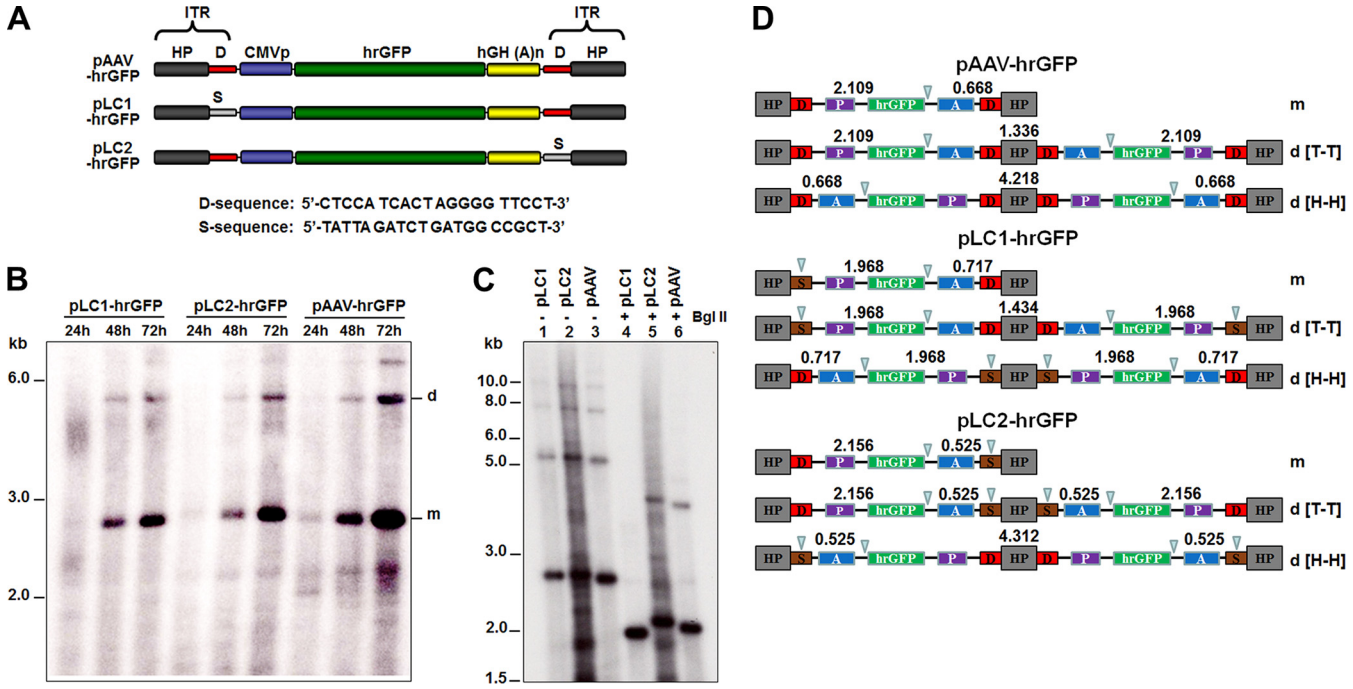

FIG 1 Effect of one D-sequence substitution on viral genome rescue and replication. (A) Schematic structures of recombinant AAV genomes. HP, hairpin structure; D, D sequence; S, substitute sequence; CMVp, cytomegalovirus promoter; hrGFP, humanized recombinant green fluorescent protein; hGH(A)n, human growth hormone poly(A) signal. (B) Southern blot analysis for rescue and replication of AAV genomes from recombinant plasmids. (C) Southern blot analysis for the structural integrity of the replicative DNA intermediates containing substitutions in the D sequence. Following digestion with or without BglII, the DNA fragments were analyzed by neutral agarose gel electrophoresis. (D) Schematic representation of structures of the replicative DNA intermediates of recombinant AAV genomes containing substitutions in the D sequence. The monomeric (m) and dimeric (d) forms of replicative DNA intermediates, in both tail-to-tail (T-T) and head-to-head (H-H) configurations, are depicted, the BglII restriction endonuclease sites are denoted by light blue arrowheads, and the DNA fragments of the predicted sizes from each of the three plasmids are indicated. Southern blot analyses using a ^{32}P-labeled DNA probe specific for hrGFP or hGH(A)n would detect the characteristic AAV replicative DNA intermediates generated from the three indicated plasmids. Following cleavage with BglII and probing with hrGFP, pLC1-hrGFP would generate only one band of 1.968 kb, pLC-2 would generate two bands of 2.155 kb and 4.310 kb, and pAAV-hrGFP would generate two bands of 2.11 kb and 4.22 kb. Following cleavage with BglII and probing with hGH(A)n, pLC1-hrGFP would generate two bands of 0.717 kb and 1.434 kb, pLC-2 would generate only one band of 0.53 kb, and pAAV-hrGFP would generate two bands of 0.672 kb and 1.344 kb.

replicated from mutant plasmids could also undergo encapsidation into viral capsids, a standard triple-plasmid transfection protocol was used to generate rAAV vectors as described in Materials and Methods. Following digestion with Benzonase to degrade any unencapsidated DNA, equivalent volumes of virus stocks were deproteinized to release the rAAV genome and 2-fold serial dilutions were analyzed on quantitative DNA slot blots using a ^{32}P-labeled hrGFP DNA probe. These results, shown in Fig. 2A, demonstrate that the presence of one D sequence in one of the two ITRs is necessary and sufficient for packaging of the AAV genome, although the vector titers appeared to be ~50% of those of the unmodified vectors, presumably because progeny strands of only [+] or [−] polarity were being encapsidated. Similar results were obtained with multiple rounds ($n = 3$ for each vector) of packaging of two different transgenes (data not shown). Analysis of the purified DNA on alkaline agarose gels revealed the same ~2.8-kb genome from all three rAAV-hrGFP vectors and no detectable linear monomers of 5.6 kb, indicating that scAAV vectors were not generated (Fig. 2B). Analysis of the denatured capsid proteins from purified viral stocks on SDS-polyacrylamide gels, followed by Western blotting, also revealed a classic VP1/VP2/VP3 protein ratio of 1:1:10 (Fig. 2C). Interestingly, however, further analyses revealed that in contrast to plasmid pAAV-hrGFP, from which ssAAV vectors of both polarities were generated as expected, the use of both mutant plasmids pLC1-hrGFP and pLC2-hrGFP led to the generation of predominantly only single-polarity vectors, as determined by using hrGFP-specific oligonucleotide probes of either [+] or [−] polarity (Fig. 2D). For the most part, the hrGFP(+) probe hybridized to the minus strand, whereas the hrGFP(−) probe hybridized to the plus strand of the viral DNA. Thus, replacement of one D sequence from one ITR leads to the generation of AAV vectors containing a single-polarity genome. These data suggest that AAV genomes containing the D[+] sequence substitution generated from both pLC1-hrGFP and pLC2-hrGFP plasmids undergo successful encapsidation, an observation also consistent with previously published reports (32, 33).

One D sequence is sufficient for replication of recombinant AAV genomes. To test whether the replacement of one D sequence affects viral DNA replication, HEK293 cells were infected with vAAV-hrGFP, vLC1-hrGFP, or vLC2-hrGFP vectors individually, followed by transfection with pHelper and pACG2 plasmids. Plasmid pAAV-hrGFP was included as an appropriate control. The viral replication intermediates were isolated at 72 h postinfection, digested with DpnI or/and BglII, and analyzed on Southern blots using ^{32}P-labeled DNA probes specific for hrGFP or poly(A) sequences, respectively. These results, shown in Fig. 3, indicated that both mutant viral genomes replicated at a level similar to that for the parental vAAV-hrGFP viral genomes.

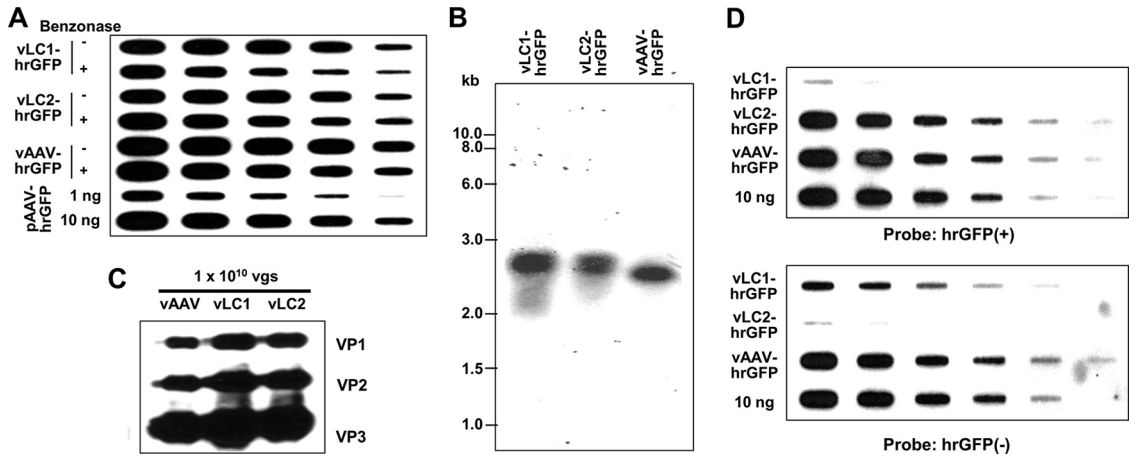

FIG 2 Effect of one D-sequence replacement on viral genome encapsidation. (A) Quantitative DNA slot blot analyses for the efficiency of packaging of the rAAV genomes from the recombinant plasmids. The titer of each rAAV vector was determined by comparison with double-stranded plasmid pAAV-hrGFP standards loaded onto the membrane. (B) Southern blot analysis of the nature of the rAAV DNA genomes in vector stocks. Equivalent volumes of DNA samples were denatured at 65°C for 30 min and electrophoresed on alkaline agarose gels. (C) Western blot analysis of denatured viral capsids from vector stocks. (D) Quantitative DNA slot blot analyses for determination of polarity of the mutant rAAV vector genomes. Two identical membranes were hybridized separately with one of the two complementary ^{32}P-labled oligonucleotides derived from the hrGFP plasmid. The hrGFP(+) (upper panel) and the hrGFP(−) (lower panel) probes hybridize with the minus strand and the plus strand of AAV DNA, respectively. The parental virus vAAV-hrGFP, which packages both strands, was included as a control.

One-D-sequence-substituted ssAAV2 vectors efficiently transduce human cells *in vitro* and murine hepatocytes *in vivo*. To evaluate the transduction efficiency of one-D-sequence-substituted ssAAV2 vectors, a panel of human cell lines was infected with each vector at 2,000 vgs/cell under identical conditions. The WT vAAV2-hrGFP vector was used as an appropriate control. As shown in Fig. 4A, in the commonly used HEK293 and HeLa cells, the mutant vectors, vLC1-hrGFP and vLC2-hrGFP, yielded ~8-fold more green fluorescence, than the WT vector. In Huh7 and U2OS cells, two cell lines less permissive for AAV2 vectors, we also observed an ~6-fold increase in the transduction efficiency. The variation in transduction efficiencies was not affected when cells were pretreated with MG132, a proteasome inhibitor, or Try23, a specific inhibitor of cellular epidermal growth factor receptor (EGFR) protein kinase (Fig. 4B), both of which are known to significantly increase the transduction efficiency of ssAAV2 vectors (13, 20), which indicates that neither intracellular trafficking nor proteasome degradation is involved. Not surprisingly, coinfection with adenovirus type 2 (Ad2) led to similar levels of increase in transgene expression mediated by the WT and the two mutant vectors in HEK293 cells (Fig. 4B), presumably because Ad2 coinfection is known to significantly increase the transduction efficiency of AAV vectors by augmenting the viral second-strand DNA synthesis, leading to optimal transgene expression (4, 5). To further confirm the role of adenoviral genes, HEK293 cells were transfected with pHelper plasmid, followed by infection with either mutant or parental viral vectors. Again, the difference between increased transduction efficiencies was not significant (Fig. 4C). On the other hand, two other plasmids, pACG2, which expresses AAV2 Rep and Cap proteins, and pRep78, which expresses only Rep 78 but no Cap proteins, had no effect. In order to obtain more quantitative data, we also performed flow cytometric analysis using both HeLa and HEK293 cells. As can be seen in Fig. 4D and E, both the GFP positivity and the mean fluorescence values were increased in both vLC1-hrGFP- and vLC2-hrGFP-infected cells compared with vAAV-hrGFP-infected cells. Quantitative analyses of the flow cytometric data for GFP expression mediated by these vectors in HeLa (Fig. 4F) and HEK293 (Fig. 4G) cells are also shown.

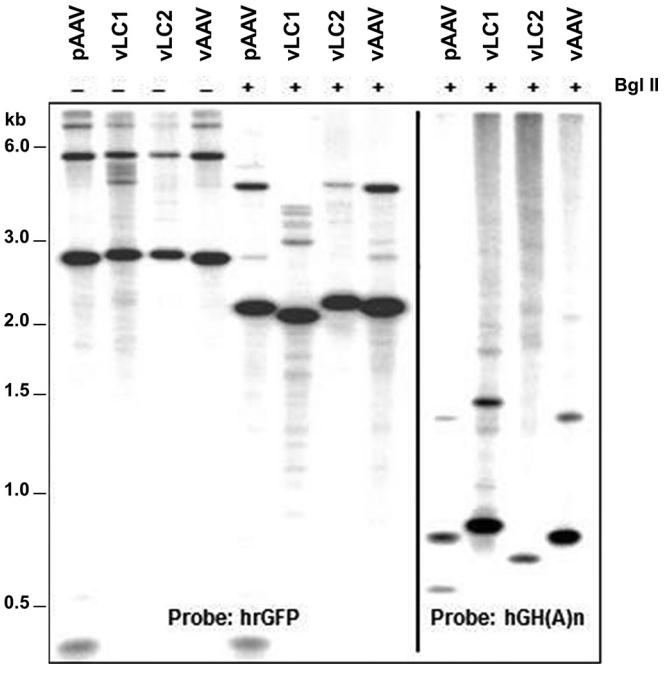

FIG 3 Southern blot analyses of replicative DNA intermediates containing substitutions in the D sequence. HEK293 cells were infected with equal amounts of vLC1-, vLC2-, or vAAV-hrGFP virions, followed by transfection with plasmids pACG2 and pHelper. Low-M_r DNA was isolated at 72 h posttransfection. DNA, with or without BglII digestion, was then separated by neutral agarose gel electrophoresis, followed by hybridization with ^{32}P-labled DNA probes specific either for hrGFP (left panel) or for hGH(A)n (right panel).

The efficacies of one-D-sequence-substituted vLC2-hrGFP

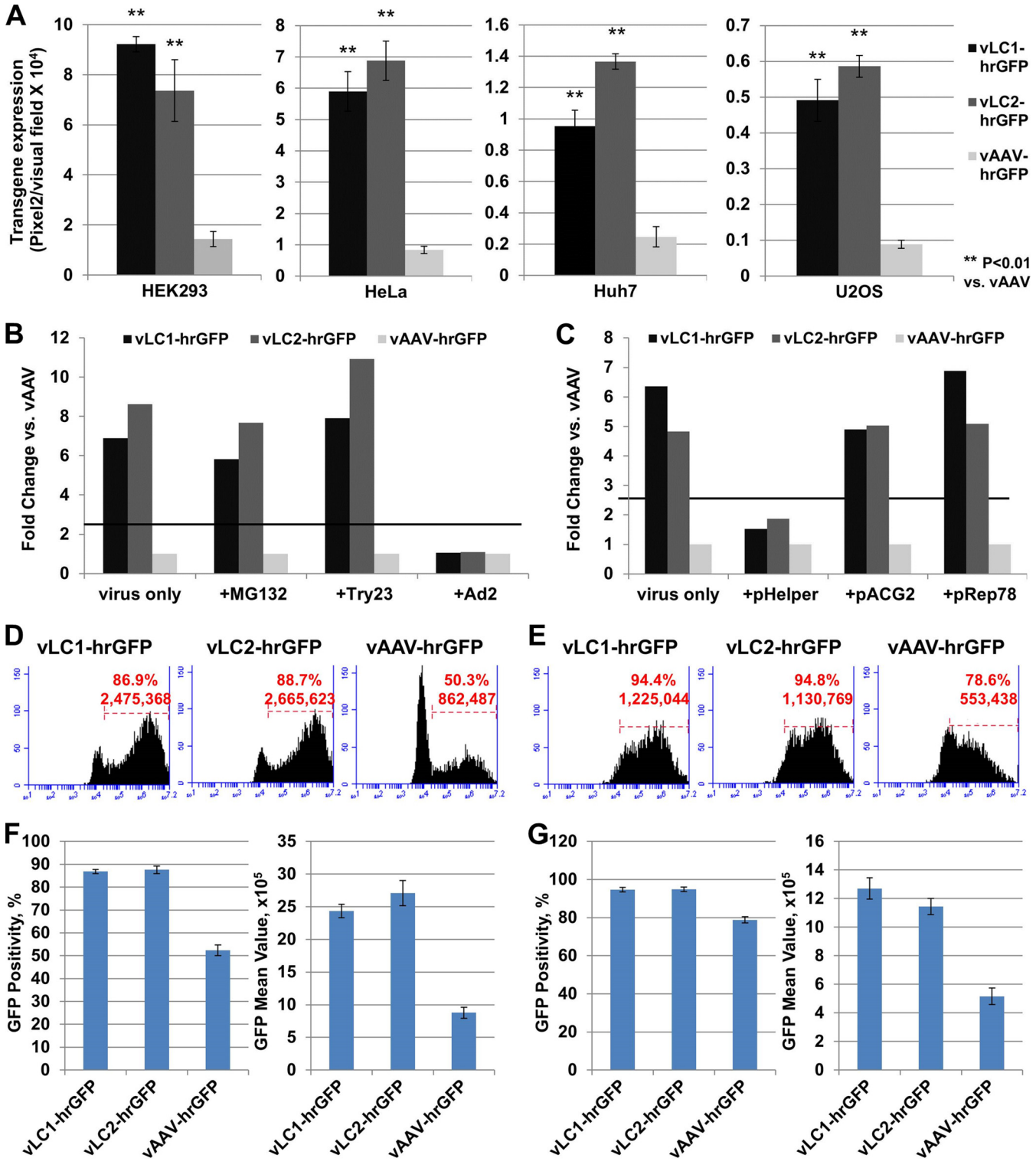

FIG 4 Transduction efficiency of one-D-sequence-substituted recombinant AAV vectors *in vitro*. (A) Comparison of transduction efficiencies of vLC1-, vLC2-, and vAAV-hrGFP vectors in permissive cell lines (HEK293 and HeLa) and in less permissive cell lines (Huh7 and U2OS). Cells were infected with viral vectors at 2,000 vgs/cell for 2 h. Transgene expression was determined by fluorescence microscopy at 72 h posttransduction. (B and C) Fold changes in transgene expression mediated by vLC1-, vLC2-, and vAAV-hrGFP vectors in HEK293 cells. Cells were infected with viral vectors at 2,000 vgs/cell for 2 h, together with treatment with chemicals or coinfection with adenovirus 2 (B) or transfection with the indicated plasmids (C). Transgene expression was determined by fluorescence microscopy at 72 h posttransduction. A change of 2.5-fold (horizontal line) was considered greater than the variability of the assay. (D and E) Transduction efficiencies of vAAV-hrGFP, vLC1-hrGFP, and vLC2-hrGFP vectors in HeLa (D) and HEK293 (E) cells. Cells were transduced with the vectors at 2,500 vgs/cell for 4 h under identical conditions, and transgene expression was determined by flow cytometry at 72 h posttransduction. Both EGFP positivity and mean fluorescence values are shown in red. (F and G) Representative flow cytometry data from each group ($n = 3$ for each cell type) for HeLa (F) and HEK293 (G) cells.

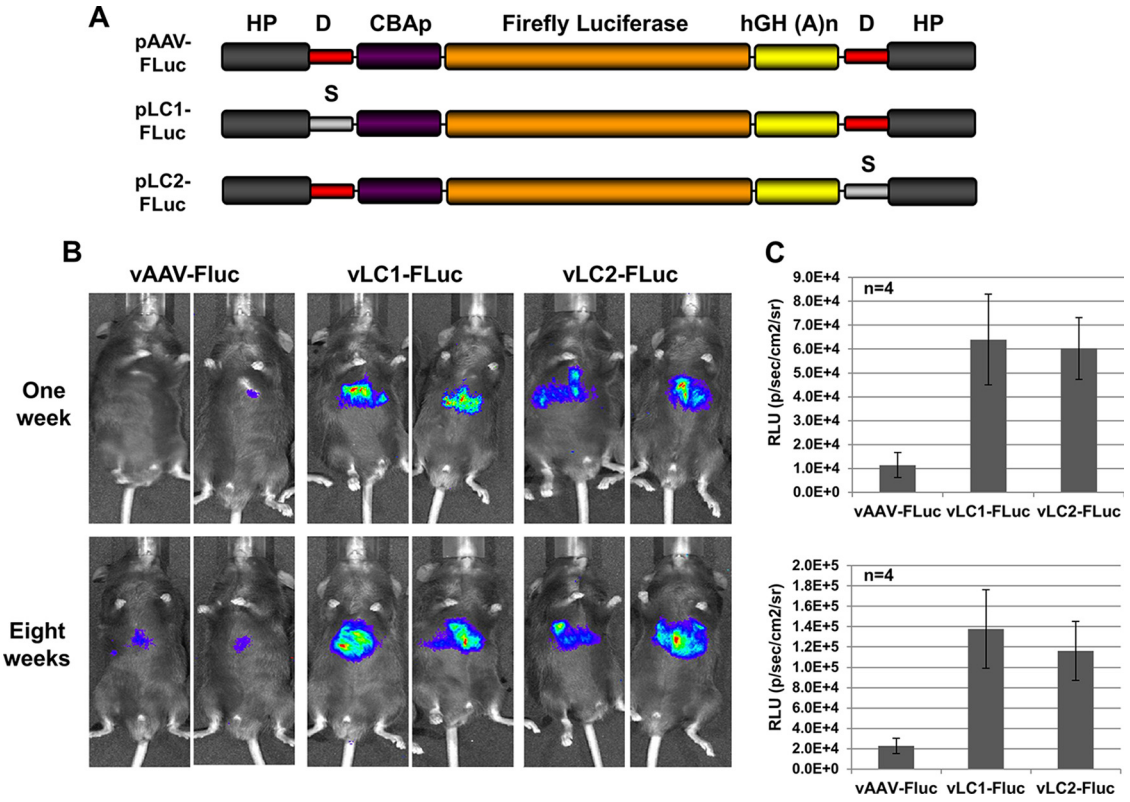

FIG 5 Transduction efficiency of one-D-sequence-substituted recombinant AAV vectors *in vivo*. (A) Schematic structures of recombinant AAV vector plasmids. CBAp, chicken β-actin promoter. (B) Bioluminescence imaging of mice injected with AAV2-Fluc vectors. C57BL/6J mice were injected with 1×10^{10} vgs of either vAAV-Fluc (left panels), vLC1-Fluc (middle panels), or vLC2-Fluc (right panels). Images were acquired with a Xenogen IVIS imaging system at 1 week or 8 weeks postinjection. Images of two representative animals from each group are shown. (C) The luminescence signal intensity was quantified as photons/second/cm^2/steridian using the Living Image software.

vector and the parental vAAV-hrGFP vectors were evaluated in a mouse model *in vivo*. C57BL/6J mice were injected via the tail vein with 1×10^{10} vgs of each viral vector. Up to 6 weeks postinjection, vAAV-hrGFP transduction was low and restricted to a small fraction of the hepatocytes, which is consistent with previous observations (15). The transduction efficiency of vLC2 vectors was significantly higher even at 2 weeks (data not shown). To more accurately determine the transgene expression levels, persistence of expression, and anatomical localization of the delivered transgenes in individual animals over time, we generated recombinant WT and D-sequence-substituted ssAAV2-firefly luciferase (Fluc) vectors under the control of the chicken β-actin promoter (CBAp). The CBAp was used to avoid promoter shutoff, a known issue to which the CMV promoter in AAV vector is prone in the liver (34). Approximately 1×10^{10} vgs of vAAV-Fluc, vLC1-Fluc, and vLC2-Fluc vectors (Fig. 5A) were injected via the tail vein in C57BL/6J mice. Whole-body bioluminescence images (Fig. 5B), acquired as detailed in Materials and Methods at either 1 or 8 weeks postinjection, also corroborated that whereas little transgene expression occurred in mice injected with the WT vAAV-Fluc vectors, expression from both mutant vectors, vLC1-Fluc and vLC2-Fluc, was up to 6-fold higher (Fig. 5C). These data demonstrate that the one-D-sequence-substituted ssAAV vectors mediate accelerated and robust transgene expression compared to the conventional ssAAV vectors in murine hepatocytes *in vivo*.

DISCUSSION

The unique structure of the 145-nt-long AAV ITR has been intriguing, since only the terminal 125 nt fold over to form a T-shaped hairpin, which at a first glance would appear to suffice for the priming of replication of the ssAAV genome, but the ITR also contains a stretch of 20 nt, designated the D sequence, which is single stranded. Nearly 2 decades ago, we and others embarked upon investigations to delineate the precise role of the D sequence in the life cycle of WT AAV2 and documented that it plays a pivotal role in AAV genome rescue, replication, packaging, and integration (18–20, 32, 33). However, the fundamental question related to the underlying mechanisms of the involvement of the D sequence in transgene expression from rAAV vectors remained unanswered. The subsequent realization that the two D sequences in a rAAV genome were not identical, but in fact were complementary to each other, and that the ssD[−] sequence was always present at the 3′ end and the ssD[+] sequence was invariably present at the 5′ end of the viral genome prompted us to explore the possibility of the existence of putative host cell proteins which might interact with these sequences.

Indeed, using both ssD[−]- and ssD[+]-sequence probes in electrophoretic mobility shift assays (EMSAs), we were able to identify two distinct cellular proteins that formed specific complexes with the ssD[−] and the ssD[+] sequences, respectively (6). In an extensive set of experiments, we identified the ssD[−]-

sequence-binding protein (13) and characterized the crucial role that it plays in modulating the viral second-strand DNA synthesis (6, 7, 13–16, 35, 36). The identity of the ssD[+]-sequence-binding protein was also revealed recently (17) as a negative regulator of transcription. These observations that proteins binding with the two D sequences at each end of a viral genome are both involved in the inhibition of transgene expression led to the systematic studies described here. The experimental data shown in Fig. 4 and 5 suggested that the replacement of one D sequence partially relieves this negative regulation. In this context, it is important to note that in our previously published studies (32, 33), in which we deleted 18 nt of the D sequence, we did not observe any increase in the transduction efficiency of these vectors. In the current studies, not only was the entire 20-nt D sequence deleted but it was replaced with a non-AAV substitute (S) sequence. Since we consistently observed improved transduction of these vectors in a number of human cell lines *in vitro*, as well as in murine hepatocytes *in vivo*, it was important to gain a better understanding of the observed differences from our previously published studies. To this end, we performed computational analyses of both the D sequence and the S sequence using the databases available at chip-mapper.org and http://www.cbrc.jp/research/db/TFSEARCH.html (37, 38), which allow the identification of putative transcription factor-binding sites in DNA genomes. These results revealed that the deletion of 18 nt from the D sequence leads to the loss of putative binding sites for 2 transcription factors (Sry-delta and Nkx2-1), whereas insertion of the S sequence provides putative binding sites for 2 transcription factors (Foxd3 and NF-muE1). Thus, the net result is not only the loss of a negative regulator of transcription (NRF) but also the gain of 2 positive regulators of transcription in the D-sequence-substituted AAV vectors, which provides a plausible explanation as to why the vectors that have 18nts deleted from the D sequence do not show superior transduction, whereas the S-sequence-substituted AAV vectors do. A more stringent search, with a threshold score of 85, which provides a higher confidence value for binding of putative transcription factors, revealed that the D sequence contains the binding site for GATA-1, whereas the S sequence contains binding sites for both GATA-1 and GATA-2 transcription factors. Thus, the loss of GATA-1 binding from the D-sequence-deleted AAV vectors and the acquisition of GATA-1 and GATA-2 binding in the S-sequence-substituted AAV vectors provide yet another plausible explanation for the observed difference between our previously published studies (32, 33) and those described here. It should be emphasized, however, that these explanations are based on theoretical computation only, and thus additional studies involving the use of electrophoretic mobility shift assays (EMSAs) are warranted to further corroborate this contention.

Together, these observations raise an interesting existential question. Why, unlike all other DNA genome-containing organisms, does the WT AAV remain single-stranded? One plausible answer is that in order to maintain its cryptic life cycle, AAV must exert enormous efforts to ensure that little viral gene expression occurs in the absence of a helper virus. We would like to suggest that the WT AAV does so by employing a "dual safety net." In the first instance, the D[−] sequence is utilized to provide the binding site for a host cell protein, FKBP52, phosphorylated forms of which strongly inhibit the viral second-strand DNA synthesis (13), since the extent of viral second-strand DNA synthesis correlates directly with the efficiency of viral gene expression. In the second instance, and in the event that some cell types might allow even a low-level conversion to transcriptionally active double-stranded viral genomes, AAV employs the D[+] sequence to negatively regulate viral gene expression. How such a negative effect is rescued by the presence of adenoviral gene products, as shown in Fig. 4B and C, warrants further studies.

Given these built-in features, it would appear that the WT single-stranded AAV is less than ideal to be used as a recombinant vector for gene therapy to achieve high-level transgene expression. Our initial attempts to develop rAAV vectors devoid of both of the D sequences in one rAAV genome did not succeed, as these genomes failed to undergo encapsidation into rAAV capsids (18–20). In the present studies, however, in which we deleted only one of the two D sequences in two respective plasmids, abundant rescue followed by replication and encapsidation of the viral genomes ensued, albeit at ~50% efficiency because only single-polarity S-sequence-substituted progeny AAV genomes are generated and packaged, in contrast to their unmodified counterparts, which are known to generate and encapsidate progeny strands of both polarities that are packaged in mature particles with equal frequency.

In sum, the studies described here, in addition to providing insights into the basic biology of AAV, also provide a means to achieve augmented transgene expression from a conventional ssAAV vector by simply deleting the D sequence in the right ITR. Given the fact that this strategy has also been successful using AAV serotype 3 vectors (unpublished data), we believe that it should be applicable to any conventional ssAAV serotype vector. Furthermore, combining these strategies with our recently described next generation of AAV vectors containing mutations in surface-exposed tyrosine, serine, and threonine residues (39–41) should further augment the transduction efficiency of all conventional ssAAV vectors for their potential use in human gene therapy.

ACKNOWLEDGMENTS

We thank Kenneth I. Berns and Sergei Zolotukhin for a critical review of the manuscript.

This research was supported in part by grants from the NIH/NCATS Clinical and Translational Science Award to the University of Florida UL1 TR000064, Alex's Lemonade Stand Foundation for Childhood Cancer, and the Bankhead-Coley Cancer Research Program (to C.L.); the National Natural Science Foundation of China (30730114); and Public Health Service grants P01 DK-058327 (Project 1), R01 HL-097088, and R21 EB-015684 from the National Institutes of Health (to A.S.). L.W. was supported by a Fellowship Award from the Government of China, and G.R.J. was supported in part by an "Overseas Associate Fellowship-2006" from the Department of Biotechnology, Government of India.

REFERENCES

1. **Srivastava A, Lusby EW, Berns KI.** 1983. Nucleotide sequence and organization of the adeno-associated virus 2 genome. J Virol **45:**555–564.
2. **Ling CQ, Wang LN, Wang Y, Zhang YH, Yin ZF, Wang M, Ling C.** 2014. The roles of traditional Chinese medicine in gene therapy. J Integr Med **12:**67–75. http://dx.doi.org/10.1016/S2095-4964(14)60019-4.
3. **Mingozzi F, High KA.** 2011. Therapeutic in vivo gene transfer for genetic disease using AAV: progress and challenges. Nat Rev Genet **12:**341–355. http://dx.doi.org/10.1038/nrg2988.
4. **Ferrari FK, Samulski T, Shenk T, Samulski RJ.** 1996. Second-strand synthesis is a rate-limiting step for efficient transduction by recombinant adeno-associated virus vectors. J Virol **70:**3227–3234.

5. **Fisher KJ, Gao GP, Weitzman MD, DeMatteo R, Burda JF, Wilson JM.** 1996. Transduction with recombinant adeno-associated virus for gene therapy is limited by leading-strand synthesis. J Virol **70:**520–532.
6. **Qing K, Wang XS, Kube DM, Ponnazhagan S, Bajpai A, Srivastava A.** 1997. Role of tyrosine phosphorylation of a cellular protein in adeno-associated virus 2-mediated transgene expression. Proc Natl Acad Sci U S A **94:**10879–10884. http://dx.doi.org/10.1073/pnas.94.20.10879.
7. **Zhong L, Chen L, Li Y, Qing K, Weigel-Kelley KA, Chan RJ, Yoder MC, Srivastava A.** 2004. Self-complementary adeno-associated virus 2 (AAV)-T cell protein tyrosine phosphatase vectors as helper viruses to improve transduction efficiency of conventional single-stranded AAV vectors in vitro and in vivo. Mol Ther **10:**950–957. http://dx.doi.org/10.1016/j.ymthe.2004.07.018.
8. **McCarty DM, Monahan PE, Samulski RJ.** 2001. Self-complementary recombinant adeno-associated virus (scAAV) vectors promote efficient transduction independently of DNA synthesis. Gene Ther **8:**1248–1254. http://dx.doi.org/10.1038/sj.gt.3301514.
9. **Wang Z, Ma HI, Li J, Sun L, Zhang J, Xiao X.** 2003. Rapid and highly efficient transduction by double-stranded adeno-associated virus vectors in vitro and in vivo. Gene Ther **10:**2105–2111. http://dx.doi.org/10.1038/sj.gt.3302133.
10. **McCarty DM, Fu H, Monahan PE, Toulson CE, Naik P, Samulski RJ.** 2003. Adeno-associated virus terminal repeat (TR) mutant generates self-complementary vectors to overcome the rate-limiting step to transduction in vivo. Gene Ther **10:**2112–2118. http://dx.doi.org/10.1038/sj.gt.3302134.
11. **Nathwani AC, Tuddenham EG, Rangarajan S, Rosales C, McIntosh J, Linch DC, Chowdary P, Riddell A, Pie AJ, Harrington C, O'Beirne J, Smith K, Pasi J, Glader B, Rustagi P, Ng CY, Kay MA, Zhou J, Spence Y, Morton CL, Allay J, Coleman J, Sleep S, Cunningham JM, Srivastava D, Basner-Tschakarjan E, Mingozzi F, High KA, Gray JT, Reiss UM, Nienhuis AW, Davidoff AM.** 2011. Adenovirus-associated virus vector-mediated gene transfer in hemophilia B. N Engl J Med **365:**2357–2365. http://dx.doi.org/10.1056/NEJMoa1108046.
12. **Wu J, Zhao W, Zhong L, Han Z, Li B, Ma W, Weigel-Kelley KA, Warrington KH, Srivastava A.** 2007. Self-complementary recombinant adeno-associated viral vectors: packaging capacity and the role of rep proteins in vector purity. Hum Gene Ther **18:**171–182. http://dx.doi.org/10.1089/hum.2006.088.
13. **Qing K, Hansen J, Weigel-Kelley KA, Tan M, Zhou S, Srivastava A.** 2001. Adeno-associated virus type 2-mediated gene transfer: role of cellular FKBP52 protein in transgene expression. J Virol **75:**8968–8976. http://dx.doi.org/10.1128/JVI.75.19.8968-8976.2001.
14. **Qing K, Li W, Zhong L, Tan M, Hansen J, Weigel-Kelley KA, Chen L, Yoder MC, Srivastava A.** 2003. Adeno-associated virus type 2-mediated gene transfer: role of cellular T-cell protein tyrosine phosphatase in transgene expression in established cell lines in vitro and transgenic mice in vivo. J Virol **77:**2741–2746. http://dx.doi.org/10.1128/JVI.77.4.2741-2746.2003.
15. **Jayandharan GR, Zhong L, Sack BK, Rivers AE, Li M, Li B, Herzog RW, Srivastava A.** 2010. Optimized adeno-associated virus (AAV)-protein phosphatase-5 helper viruses for efficient liver transduction by single-stranded AAV vectors: therapeutic expression of factor IX at reduced vector doses. Hum Gene Ther **21:**271–283. http://dx.doi.org/10.1089/hum.2009.100.
16. **Zhao W, Wu J, Zhong L, Srivastava A.** 2007. Adeno-associated virus 2-mediated gene transfer: role of a cellular serine/threonine protein phosphatase in augmenting transduction efficiency. Gene Ther **14:**545–550. http://dx.doi.org/10.1038/sj.gt.3302886.
17. **Jayandharan GR, Aslanidi G, Martino AT, Jahn SC, Perrin GQ, Herzog RW, Srivastava A.** 2011. Activation of the NF-kappaB pathway by adeno-associated virus (AAV) vectors and its implications in immune response and gene therapy. Proc Natl Acad Sci U S A **108:**3743–3748. http://dx.doi.org/10.1073/pnas.1012753108.
18. **Wang XS, Ponnazhagan S, Srivastava A.** 1995. Rescue and replication signals of the adeno-associated virus 2 genome. J Mol Biol **250:**573–580. http://dx.doi.org/10.1006/jmbi.1995.0398.
19. **Wang XS, Ponnazhagan S, Srivastava A.** 1996. Rescue and replication of adeno-associated virus type 2 as well as vector DNA sequences from recombinant plasmids containing deletions in the viral inverted terminal repeats: selective encapsidation of viral genomes in progeny virions. J Virol **70:**1668–1677.
20. **Wang XS, Qing K, Ponnazhagan S, Srivastava A.** 1997. Adeno-associated virus type 2 DNA replication in vivo: mutation analyses of the D sequence in viral inverted terminal repeats. J Virol **71:**3077–3082.
21. **Ling C, Lu Y, Kalsi JK, Jayandharan GR, Li B, Ma W, Cheng B, Gee SW, McGoogan KE, Govindasamy L, Zhong L, Agbandje-McKenna M, Srivastava A.** 2010. Human hepatocyte growth factor receptor is a cellular coreceptor for adeno-associated virus serotype 3. Hum Gene Ther **21:**1741–1747. http://dx.doi.org/10.1089/hum.2010.075.
22. **Hirt B.** 1967. Selective extraction of polyoma DNA from infected mouse cell cultures. J Mol Biol **26:**365–369. http://dx.doi.org/10.1016/0022-2836(67)90307-5.
23. **Wang LN, Wang Y, Lu Y, Yin ZF, Zhang YH, Aslanidi GV, Srivastava A, Ling CQ, Ling C.** 2014. Pristimerin enhances recombinant adeno-associated virus vector-mediated transgene expression in human cell lines in vitro and murine hepatocytes in vivo. J Integr Med **12:**20–34. http://dx.doi.org/10.1016/S2095-4964(14)60003-0.
24. **Liu Y, Joo KI, Wang P.** 2013. Endocytic processing of adeno-associated virus type 8 vectors for transduction of target cells. Gene Ther **20:**308–317. http://dx.doi.org/10.1038/gt.2012.41.
25. **Ling C, Lu Y, Cheng B, McGoogan KE, Gee SW, Ma W, Li B, Aslanidi GV, Srivastava A.** 2011. High-efficiency transduction of liver cancer cells by recombinant adeno-associated virus serotype 3 vectors. J Vis Exp http://dx.doi.org/10.3791/2538.
26. **Dai Y, Bae K, Siemann DW.** 2011. Impact of hypoxia on the metastatic potential of human prostate cancer cells. Int J Radiat Oncol Biol Phys **81:**521–528. http://dx.doi.org/10.1016/j.ijrobp.2011.04.027.
27. **Gu Y, Lin S, Li JL, Nakagawa H, Chen Z, Jin B, Tian L, Ucar DA, Shen H, Lu J, Hochwald SN, Kaye FJ, Wu L.** 2012. Altered LKB1/CREB-regulated transcription co-activator (CRTC) signaling axis promotes esophageal cancer cell migration and invasion. Oncogene **31:**469–479. http://dx.doi.org/10.1038/onc.2011.247.
28. **Dong B, Nakai H, Xiao W.** 2010. Characterization of genome integrity for oversized recombinant AAV vector. Mol Ther **18:**87–92. http://dx.doi.org/10.1038/mt.2009.258.
29. **Wu Z, Yang H, Colosi P.** 2010. Effect of genome size on AAV vector packaging. Mol Ther **18:**80–86. http://dx.doi.org/10.1038/mt.2009.255.
30. **Lai Y, Yue Y, Duan D.** 2010. Evidence for the failure of adeno-associated virus serotype 5 to package a viral genome > or = 8.2 kb. Mol Ther **18:**75–79. http://dx.doi.org/10.1038/mt.2009.256.
31. **Samulski RJ, Srivastava A, Berns KI, Muzyczka N.** 1983. Rescue of adeno-associated virus from recombinant plasmids: gene correction within the terminal repeats of AAV. Cell **33:**135–143. http://dx.doi.org/10.1016/0092-8674(83)90342-2.
32. **Zhou X, Zeng X, Fan Z, Li C, McCown T, Samulski RJ, Xiao X.** 2008. Adeno-associated virus of a single-polarity DNA genome is capable of transduction in vivo. Mol Ther **16:**494–499. http://dx.doi.org/10.1038/sj.mt.6300397.
33. **Zhong L, Zhou X, Li Y, Qing K, Xiao X, Samulski RJ, Srivastava A.** 2008. Single-polarity recombinant adeno-associated virus 2 vector-mediated transgene expression in vitro and in vivo: mechanism of transduction. Mol Ther **16:**290–295. http://dx.doi.org/10.1038/sj.mt.6300376.
34. **Papadakis ED, Nicklin SA, Baker AH, White SJ.** 2004. Promoters and control elements: designing expression cassettes for gene therapy. Curr Gene Ther **4:**89–113. http://dx.doi.org/10.2174/1566523044578077.
35. **Qing K, Khuntirat B, Mah C, Kube DM, Wang XS, Ponnazhagan S, Zhou S, Dwarki VJ, Yoder MC, Srivastava A.** 1998. Adeno-associated virus type 2-mediated gene transfer: correlation of tyrosine phosphorylation of the cellular single-stranded D sequence-binding protein with transgene expression in human cells in vitro and murine tissues in vivo. J Virol **72:**1593–1599.
36. **Mah C, Qing K, Khuntirat B, Ponnazhagan S, Wang XS, Kube DM, Yoder MC, Srivastava A.** 1998. Adeno-associated virus type 2-mediated gene transfer: role of epidermal growth factor receptor protein tyrosine kinase in transgene expression. J Virol **72:**9835–9843.
37. **Heinemeyer T, Wingender E, Reuter I, Hermjakob H, Kel AE, Kel OV, Ignatieva EV, Ananko EA, Podkolodnaya OA, Kolpakov FA, Podkolodny NL, Kolchanov NA.** 1998. Databases on transcriptional regulation: TRANSFAC, TRRD and COMPEL. Nucleic Acids Res **26:**362–367. http://dx.doi.org/10.1093/nar/26.1.362.
38. **Marinescu VD, Kohane IS, Riva A.** 2005. MAPPER: a search engine for the computational identification of putative transcription factor binding sites in multiple genomes. BMC Bioinformatics **6:**79. http://dx.doi.org/10.1186/1471-2105-6-79.

39. **Markusic DM, Herzog RW, Aslanidi GV, Hoffman BE, Li B, Li M, Jayandharan GR, Ling C, Zolotukhin I, Ma W, Zolotukhin S, Srivastava A, Zhong L.** 2010. High-efficiency transduction and correction of murine hemophilia B using AAV2 vectors devoid of multiple surface-exposed tyrosines. Mol Ther **18:**2048–2056. http://dx.doi.org/10.1038/mt.2010.172.
40. **Aslanidi GV, Rivers AE, Ortiz L, Govindasamy L, Ling C, Jayandharan GR, Zolotukhin S, Agbandje-McKenna M, Srivastava A.** 2012. High-efficiency transduction of human monocyte-derived dendritic cells by capsid-modified recombinant AAV2 vectors. Vaccine **30:**3908–3917. http://dx.doi.org/10.1016/j.vaccine.2012.03.079.
41. **Aslanidi GV, Rivers AE, Ortiz L, Song L, Ling C, Govindasamy L, Van Vliet K, Tan M, Agbandje-McKenna M, Srivastava A.** 2013. Optimization of the capsid of recombinant adeno-associated virus 2 (AAV2) vectors: the final threshold? PLoS One **8:**e59142. http://dx.doi.org/10.1371/journal.pone.0059142.